



Journal of Mechanics of Materials and Structures

AXIAL COMPRESSION OF HOLLOW ELASTIC SPHERES

Robert Shorter, John D. Smith, Vincent A. Coveney and James J. C. Busfield

Volume 5, No. 5

May 2010



mathematical sciences publishers

AXIAL COMPRESSION OF HOLLOW ELASTIC SPHERES

ROBERT SHORTER, JOHN D. SMITH, VINCENT A. COVENEY AND JAMES J. C. BUSFIELD

When thin-walled hollow elastic spheres are compressed between two parallel rigid surfaces, there is an initial flattening of the sphere in the contact regions, followed by a snap-through buckling of the flattened surface. As the compression increases the sphere undergoes further buckling modes as a number of ridges and folds are formed. This elastic buckling deformation is investigated using a finite element analysis (FEA) technique. It is shown that the ratio of displacement at buckling to wall thickness depends weakly not only on Poisson's ratio, ν , but also on the ratio of the geometric wall thickness, h , to sphere radius, R . This approach is validated by comparison with experimental compression results on microspheres of approximately $40\ \mu\text{m}$ in diameter to table tennis balls with a diameter of 40 mm.

The analysis shows that a simple axial compression of a thin-walled hollow sphere can be used to measure both the average wall thickness of the sphere, from the deformation at the buckling snap-through, and the modulus from the force at this point. This provides a good technique to fully characterise the geometry and the elastic behaviour of thin-walled spheres of any size.

Introduction

Hollow thin-walled spheres are used for a variety of applications ranging from the recreational (table tennis balls, tennis balls, footballs), the industrial (lightweight and syntactic foams), through to the medical (the use of ultrasonic contrast agents to enhance ultrasonic imaging). In many of these applications the mechanical properties of the spherical shell play an important role, yet reliable measurements of those properties are often difficult to obtain. For example, with sintered foam structures made from hollow spheres, such as that proposed in [Taguchi and Karushige 2007; Peng et al. 2000], it is important that the mechanical properties of the individual spheres are known. With polymer spheres, even if samples of the polymer constituent are available, the manufacturing method may influence the final mechanical properties. This is often the case for example with polymers made by blow or injection moulding where an in-situ measurement may be desirable.

The situation is even starker for microscopic fillers: for example, with ultrasonic contrast agents where experimental evidence indicates that the elasticity and thickness of the shell are important components to the overall dynamics [Leong-Poi et al. 2002; Ketterling et al. 2007]. Such shells often have a diameter of a few μm and are constructed of proteins and lipids. Another type of hollow sphere, commercially available as Expancel[®] microspheres, are encountered in industrial applications as either a way of reducing weight or to act as a blowing agent. These range in diameter from 20 to $55\ \mu\text{m}$ with shell thicknesses of approximately $0.1\ \mu\text{m}$. In [Trivett et al. 2006], when the behaviour of these microspheres was studied in castor oil, the Young's modulus of the shell was estimated to be $\sim 3\ \text{GPa}$ from the sound speed of the

Keywords: compression, buckling, instability, hollow spheres, finite element analysis,

mixture, but in this case the spheres are formed by a chemical reaction in-situ and it is not possible to obtain a test sample of the shell polymer to confirm this estimate.

The axial compression of either hollow hemispheres and spheres between parallel rigid planes has been studied in [Updike and Kalnins 1970; 1972; Taber 1983; Pauchard and Rica 1998]. In the first of these references an axisymmetric elastic solution was developed and it was shown that during compression the initial response is to form a flat surface followed at larger deformations by a buckled solution. Updike and Kalnins [1972] extended this work to larger displacements and derived a solution that indicates that a nonsymmetric solution exists where contact lobes are formed on the contact ring. Taber [1983] tackled the problem of what happens if the sphere is filled with a pressurised fluid. It was found experimentally in [Pauchard and Rica 1998] that, for low applied forces, the shell flattens against the surfaces as predicted in [Updike and Kalnins 1970]. As the force is increased the shell suddenly buckled when the deformation was close to twice the thickness of the shell. Using the Föppl–von Kármán theory for thick shells [Föppl 1907, § 24, pp. 132–144; Ben and Pomeau 1997; Pomeau 1998], together with the observed configuration of the deformation, Pauchard and Rica deduced the form of the energy of an axially symmetric deformed spherical shell. This expression qualitatively explains the observed features but it contains a set of unknown parameters that, on dimensional grounds, are only expected to depend on the Poisson's ratio of the shell material. In this paper these various earlier approaches are re-examined using a finite-element analysis (FEA) numerical investigation into the dependence of the buckling transition and associated force-deflection curve on the material and geometric properties. It is shown that the ratio of displacement at buckling to wall thickness depends weakly not only on Poisson's ratio but also weakly on the geometric wall thickness to sphere radius ratio as well.

The precise form of the force-deflection curve before buckling is also found to be dependent on Poisson's ratio, the sphere geometry and the modulus. It should therefore be possible to derive master curves of buckling force and displacement at specified Poisson's ratios which can then be used to determine the Young's modulus and thickness of a sphere, from a measurement of the force at a specified displacement together with the displacement at the point of the buckling instability. This is clearly a very useful extension of previous work. The theory is tested here using experimental results measured during the axial compression of table tennis balls and Expancel microspheres.

1. Theory

Pauchard and Rica [1998] considered the contact of a spherical shell with a rigid plate. Before buckling, the situation is assumed to conform to Configuration I of Figure 1, in which the top and bottom contact surface of the sphere flatten against the flat rigid plates, the total deflection being $2x$. After buckling it is assumed that the deformed sections of the sphere invert and the situation corresponds to Configuration II in the figure. The theory used to derive our dimensional approach is given in the Appendix. The displacements here are expressed as a dimensionless term given as the ratio of the deflection to the thickness ratio of the shell, $\varepsilon = x/h$.

Equation (A-3) implies that the scaled displacement to buckle the shell, ε_b is expected to depend only on Poisson's ratio and is independent of the Young's modulus and the size of the sphere whereas (A-5) states that the reduced force, RF/Eh^3 , is a function only of ε and Poisson's ratio. It should be noted that, if the functions f , g_I and g_{II} depend only weakly on ν , then ε_b is approximately constant and the

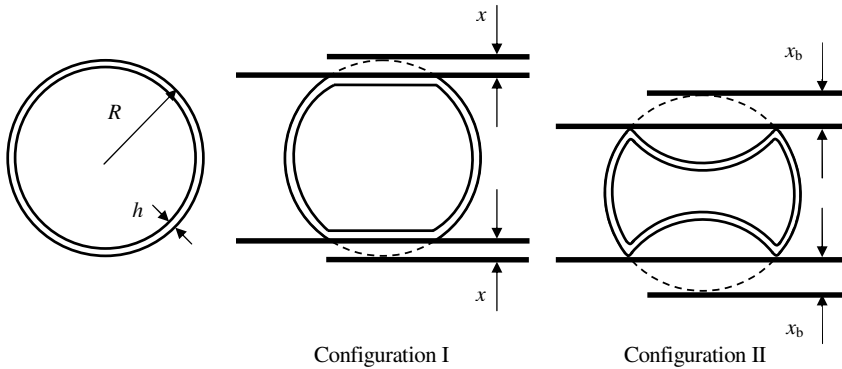


Figure 1. Assumed configurations of sphere and plate before buckling (Configuration I) and after (Configuration II).

reduced force lies on an approximately universal curve which is the same for any sphere, regardless of size or material parameters. The assumed forms of the energy expressions leading to the results (A-5) and (A-6) appear to be based on thin shell theory however the exact nature of some of the approximations is unclear. It is to be expected however that the buckling displacement arises from the root of an equation of the form of (A-3) and the reduced force will have a form similar to (A-5) however the exact functional dependence could be more complicated. This will be explored using the numerical model presented in the following section.

This paper focuses on the initial elastic buckling phenomena observed when a thin-walled shell is compressed between two rigid flat plates. An approach similar to that proposed in [Maalawi 2008] has been used to derive dimensionless functions to make the work applicable to a very wide range of conditions. In this work the measured or predicted force, F , is plotted in a normalised dimensionless form suggested by (A-5) as RF/Eh^3 and the scaled displacement is plotted as ε . Initial modelling also confirmed that the force scales directly with the applied modulus. Figure 2 shows a schematic for the full

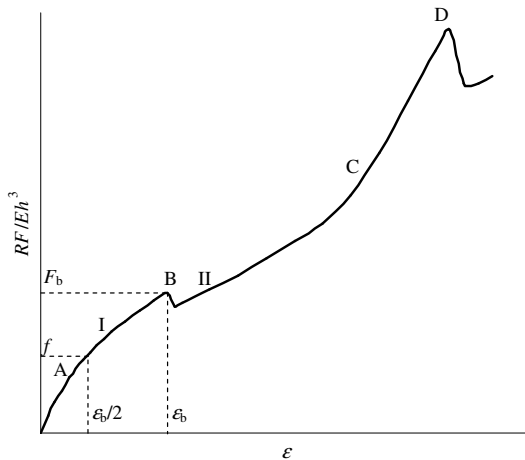


Figure 2. Schematic of the force-deflection curve for the compression of a spherical shell between two rigid plates.

compression of a hollow sphere until it is totally crushed. In the figure we are primarily concerned with the small strain initial elastic buckling behaviour. There is an initial inflexion in the curve at A: this is predicted by the form of (A-6)₁ and is associated with the dominance with increasing deformation of the energy associated with the compressed material on the flat portion of Configuration I over the energy in the fold, however it is typically more pronounced in practice. The second kink in the curve, labelled B, is the buckling instability that is the major focus of this paper. Immediately above B the sphere resembles Configuration II in Figure 1. As the displacement increases further (C) the graph stiffens further due to the onset of self contact between the internal top and bottom surfaces meeting inside the sphere. The further peaks in the force behaviour, labelled D, result from detailed buckling and folding as the sphere becomes fully compressed.

2. Numerical methods

The initial compression and buckling instability of the hollow spheres was modelled using ABAQUS finite element software. Previous studies [Kelly and Takhirov 2007] showed that ABAQUS was a suitable software package for modelling simple elastic buckling phenomena. Trials showed that the best way to model the elastic buckling behaviour required the use of the explicit dynamics package, with the time step set to model a pseudostatic analysis. Initially full three-dimensional models using solid continuum three-dimensional reduced integration (C3D8R) elements were used, a typical example of which is shown in Figure 3, left. Mesh sensitivity studies indicated that to replicate the buckling modes correctly, at least four elements had to be used through the thickness. The studies also showed that the most reproducible results were obtained for models based on elements that were approximately cubic. This put a significant demand on the model creation for thin, full three-dimensional models, as when the thinnest models were attempted it was necessary to use over 200,000 elements, which required significant solution time to solve. It was clearly possible to add the additional elements only in the regions of contact and buckling; however at large displacement the contact regions moved substantially, making it easier to use a uniform

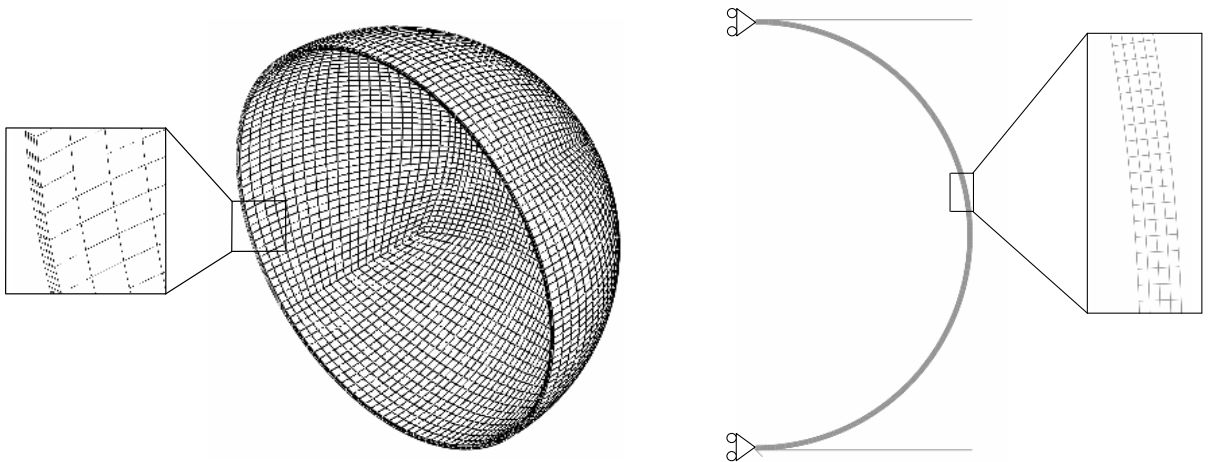


Figure 3. Left: Three-dimensional model showing mesh. Right: Axisymmetric model showing mesh and boundary conditions.

mesh. Next a model that incorporated thin shell finite elements was used. Wong and Pellegrino [2006a; 2006b] have shown that buckling phenomena of thin shell structures can in general be well modelled using this approach. However, in the case presented here this approach had difficulty resolving all the contact constraints. An alternative modelling approach that used a 2D axisymmetric model with continuum axisymmetric four node (CAX4) elements was produced. A typical model adopted is shown in Figure 3, right, with the appropriate symmetry and boundary conditions highlighted. In this case it was not computationally too expensive to use a large number of elements.

The numerical methods introduce an inherent uncertainty in the prediction of the point of instability, ϵ_b . To minimise this, a standard approach was adopted where the separation between the top contacting node in the model and the rigid surface was monitored throughout the analysis. The buckling was taken to be when the rate of change of this separation with time was at a maximum. The error in determining the maximum for a particular model is therefore determined by the discretisation of the time step and has a value of about 3%. The mesh convergence studies suggested that the errors due to meshing were much smaller and hence the overall estimate for the error is thought to be about 3%. This is the source of the error bars shown in some of the figures.

Figure 4 plots normalised buckling instability displacement ϵ_b for a range of different shell thickness to sphere radius ratios (h/R) predicted using both the three-dimensional models and the axisymmetric models for a Poisson’s ratio of 0.3. Clearly there is very little to distinguish between the two sets of results. This confirms, that at least for this initial snap-through elastic buckling, the behaviour is axisymmetric and no out of plane buckling arises that would require the use of a full three-dimensional model. It is also worth noting that the work presented here has a very similar buckling displacement to that seen in [Updike and Kalnins 1970] who reported for similar geometries a scaled buckling displacement, ϵ_b , of between 2.2 and 2.3. To speed up the analysis all the initial elastic buckling work reported in the rest of the paper uses the axisymmetric modelling approach.

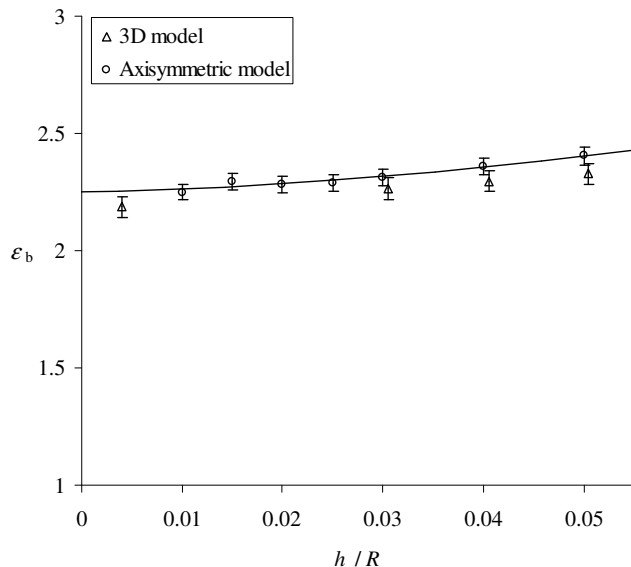


Figure 4. Snap-through deflection as a function of sphere radius when $\nu = 0.3$.

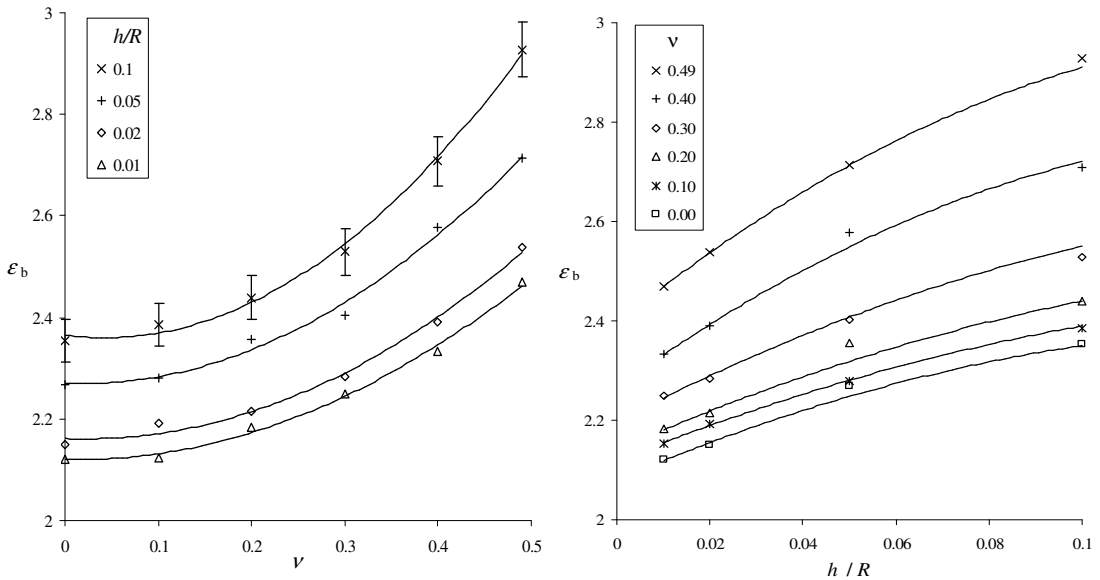


Figure 5. Left: Snap-through buckling point ε_b versus Poisson's ratio ν for a range of thickness-to-radius ratios (h/R) (left), and versus h/R for a range of values of ν (right).

The two parts of Figure 5 plot the dependence of the buckling instability displacement on the Poisson's ratio of the material and also for a wide range of ratios of wall thickness to sphere radius. Pauchard and Rica [1998] approach as given by (A-1) suggests that each of the various different geometries should superimpose to a single master curve when the buckling point is plotted against Poisson's ratio. Clearly this is not the case as there is a small but clear geometric dependence as well. Pauchard and Rica suggested a value of about 2 for ε_b and this is comparable with the values that we have derived for the thinnest spheres. It is not clear from their paper but it appears likely that their approach is only valid for very thin shells. A principal aim of this work is to produce curves to allow the wall thickness to be measured from a simple measure of the buckling displacement provided that the Poisson's ratio for the material is known.

The second aim of this paper is to use the buckling force to deduce the modulus for the sphere. However, there is a problem, as even though the actual buckling displacement was relatively insensitive to mesh shape producing errors of less than 3%, the maximum force, F_b (shown in Figure 2) achieved at this displacement was sensitive to discretisation details and produced much more significant errors of about 15%. An approach was adopted here to reduce this artefact of the modelling; this used the force, f , at the point half way to buckling, $\varepsilon_b/2$. As this point is far from the buckling instability, it is much less sensitive to small changes in the mesh geometry or the precise detail of the discretisation of the time step.

The wide range of geometric variations shown in Figure 5 are again plotted in Figure 6, but this time to show how the normalised force at half of the buckling displacement varies with Poisson's ratio and for different values of normalised wall thickness. Again, there is a clear geometric dependence that is not predicted in [Pauchard and Rica 1998]. Knowledge of this dependence, as shown in the graph,

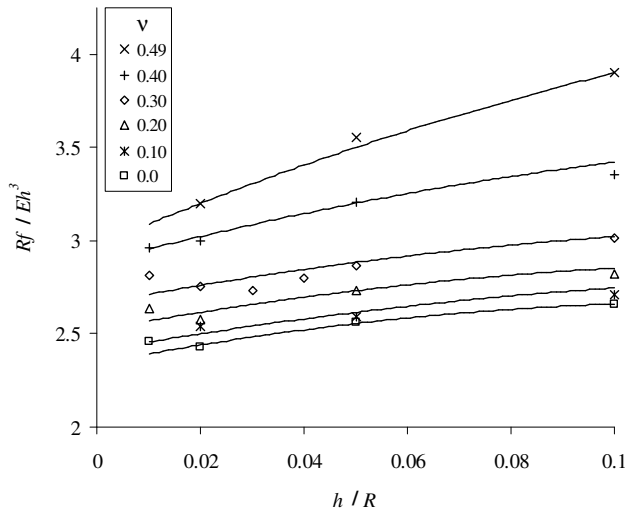


Figure 6. Normalised force versus radius. The value given is for the force at half of the buckling point, f .

allows one to identify the modulus of the sphere from a knowledge of the force at the point half way to buckling, f . Figure 6 also verifies that the data for similar geometries and Poisson’s ratio reduce to the same normalised force when modelled at different moduli.

3. Experimental comparison and discussion

Initially this theory was validated by experiments on table tennis balls, where independent measurements can be made of both the wall thickness and the modulus. Similar validation experiments were attempted on a series of Expancel spheres. It did however prove much harder to measure the modulus and experiments that tried to break open individual spheres to measure their wall thickness resulted in the spheres being damaged too extensively.

The experimental process to test the stiffness of the table tennis balls required for each ball to be placed on a flat rigid steel plate, as shown in Figure 7. Table tennis balls are manufactured in two halves with a welded seam joining the two parts. The balls were placed so that the seam was horizontal. A 1 kN load cell was used to measure the force and the displacement was measured by the movement of the crosshead which moved at a rate of 5 mm/min. The average scaled buckling displacement, ϵ_b , measured over 12 samples was 2.30. Assuming that the Poisson’s ratio was 0.3, taken from [Nakamura et al. 2004] and the measured radius for the table tennis ball of 19.85 mm \pm 0.05 mm, the prediction for the wall thickness deduced from Figure 5 was 0.42 mm. This compares well to the average experimentally measured wall thickness value of 0.40 mm \pm 0.04 mm. Similarly the average experimentally measured force at the half buckling point for the same geometry gives a prediction using Figure 6 for the modulus for the table tennis ball of 2.19 MPa.

An independent measure for the elasticity modulus was made using a dynamic mechanical thermal analyser (DMTA) on samples cut from the shells of the table tennis balls. In this machine a forced oscillation is applied with both the displacement and the force measured during the loading cycle. From this

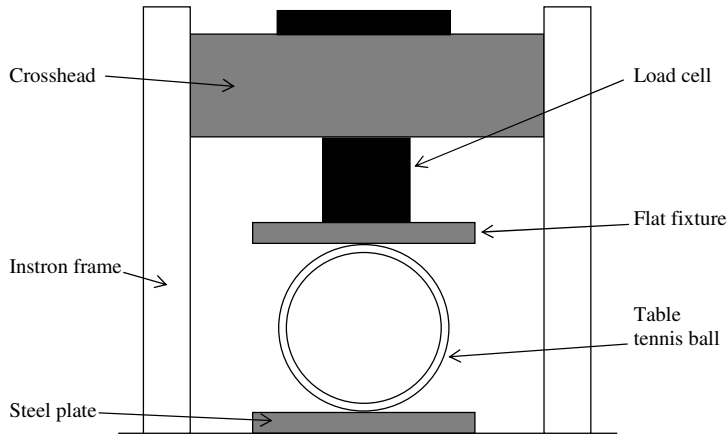


Figure 7. A schematic of the experimental setup used to measure the compression behaviour of the table tennis balls.

is derived the elastic behaviour. These properties were measured both in tension and then in three point bending. Both techniques delivered similar values for the tensile modulus of 2.2 MPa which compares very well with the value deduced from the compression experiment. Stresses taken from the model at buckling show that the maximum stresses were well below the yield stress measured at 60 MPa on a dumbbell shaped tensile test piece also cut from the table tennis ball shell.

Figure 8 plots the force versus displacement (on the appropriate dimensionless axes) from an axisymmetric model of the initial buckling of the table tennis ball with the modulus data in the model being

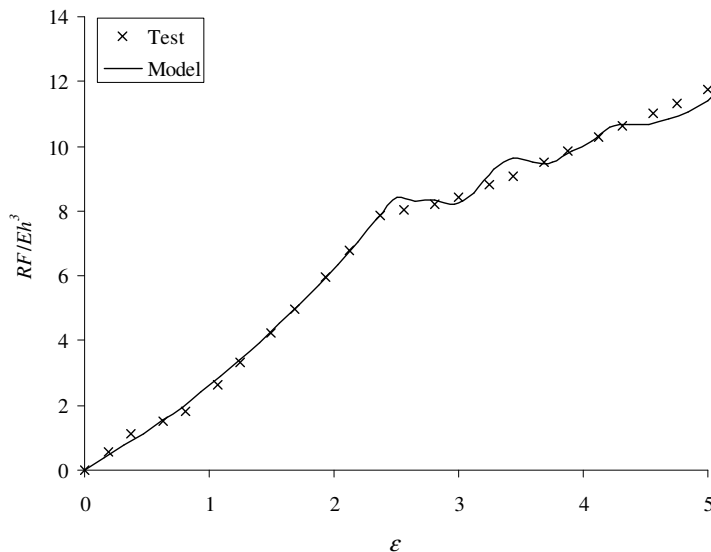


Figure 8. Finite element axisymmetric model compared to experimental compression of a table tennis ball of radius 20 mm and wall thickness 0.4 mm, FEA prediction uses a modulus of 2.2 MPa.

taken from the DMTA tests and the geometry from the measured results. This is compared with an experimentally measured data set for the compression of a table tennis ball. It is clear that the general behaviour is well predicted by the FEA approach, with the initial buckling displacement, ε_b being predicted accurately. The small oscillations observed in the model response are due to small discrete changes in the number of elements that are in contact with the rigid surfaces throughout the model. A separate model, not shown, with a realistic amount of plasticity introduced in the model, had no influence on this initial buckling phenomenon.

Next a series of different Expancel spheres were compressed using a UMIS 2000 nano-indentation machine. The machine was calibrated using the incorporated video microscope display and the X , Y coordinates set at a reference point. A small number of microspheres were placed on a microscope slide and were dispersed using distilled water, which was allowed to evaporate. The microscope slide was placed onto a specimen plinth using dental wax, which was melted at approximately 40°C and allowed to cool and set. The plinth was then placed in the nano-indentation machine and initially single microspheres were located using the video microscope display. Clearly it was important to compress just a single sphere. The indenter tip was 1 mm in diameter and made from a ruby, it was initially placed above the microsphere and allowed to stabilise for thirty minutes.

The indentation was achieved by moving the indenter tip in the $-Z$ direction by approximately 50% of the microsphere diameter. The process was repeated for a number of microspheres of differing measured diameters. Figure 9 shows the typical behaviour of the initial elastic compression of one of the microspheres with a radius of $24\ \mu\text{m}$. Assuming a Poisson's ratio of 0.3 as in [Nakamura et al. 2004], from the buckling point it is possible to identify the wall thickness to be $0.38\ \mu\text{m} \pm 0.02\ \mu\text{m}$ and from the force at the half way to buckling point the modulus was deduced as being 3.4 MPa. This gives a good indication of the values that we can expect for the wall thickness and the modulus. This will be

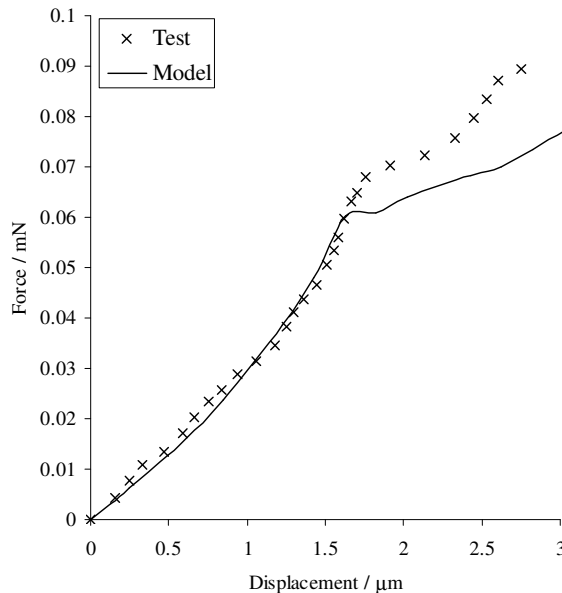


Figure 9. Experimental compression of a single microsphere ($R = 20.24\ \mu\text{m}$). The predicted curve has wall thickness $0.4\ \mu\text{m}$, modulus 3.4 MPa and Poisson's ratio 0.3.

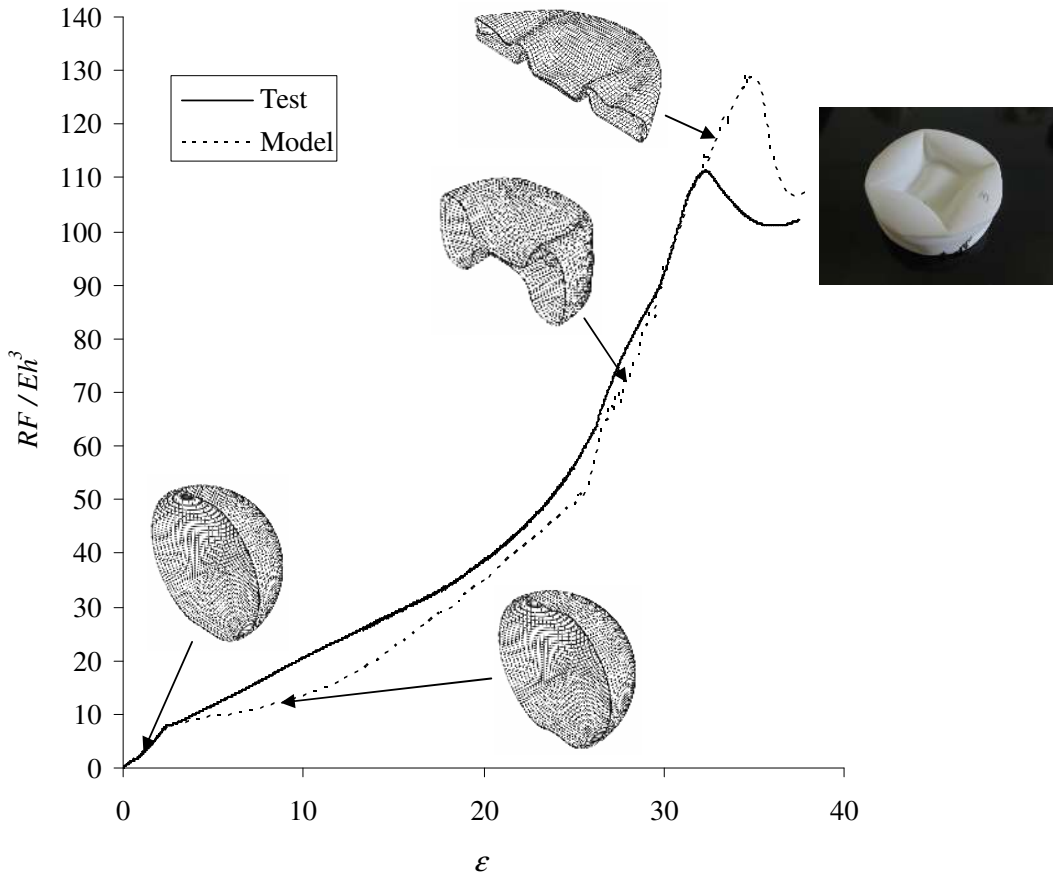


Figure 10. Finite element three-dimensional model compared to experimental compression of a table tennis ball.

particularly important in future work whereby we aim to model the influence of these microspheres on the physical properties when incorporated as a filler into rubber.

Whilst the post-buckling behaviour is beyond the scope of this paper, [Figure 10](#) shows what happens beyond the initial buckling for a table tennis ball. In this test the ball has been compressed to just 6% of the original diameter of 40 mm, between two flat rigid plates using a screw-driven Instron 5584 test machine. This experiment is compared to a full three-dimensional model, as a two-dimensional axisymmetric model gave a much stiffer post-buckling response since it constrained the model to having only symmetric buckling modes. Clearly the elastic limit for the material is exceeded in this experiment and so to get an accurate model it was necessary to model the sphere using elastoplastic behaviour. In this case the properties were derived from a tensile test strip cut from the wall of the sphere. The plastic behaviour used had an initial yield stress of 50 MPa and then the materials became perfectly plastic at a plastic strain of 0.012 and at a stress of 60 MPa. Under these conditions not only is the initial buckling predicted well but also the final folding. A model without plasticity introduced was far too stiff. The FEA model gives too soft a response in the middle range. This is most likely to result from inaccuracies associated by ignoring the weld line in the model.

4. Conclusions

The compression of a thin-walled hollow elastic sphere between two parallel rigid surfaces is predicted well using an explicit dynamics finite element analysis package. The observed initial flattening of the sphere in the contact regions, followed by a snap-through buckling of the flattened surface are all modelled well. The ratio of displacement at buckling at point *B* in Figure 2 to wall thickness was seen to not only depend weakly upon the Poisson's ratio, as predicted in [Pauchard and Rica 1998], but there was also a dependence upon the geometric wall thickness to sphere radius ratio that had not previously been reported. This approach was validated by comparison with experimental compression results on microspheres of approximately 20 μm in radius and table tennis balls with a radius of 20 mm.

The analysis shows that a simple axial compression of a thin-walled hollow sphere can be used to measure both the average wall thickness of the sphere from the deformation at the buckling snap-through and the modulus from the force at the point half way to the point of the snap-through. This provides a good technique to fully characterise the geometry and the elastic behaviour of thin-walled spheres of any size.

Acknowledgements

The authors thank Andy Bushby in the Department of Materials at QMUL, for his support and guidance in using the nano-indentation technique. One of the authors, Robert Shorter, would also like to thank DITC and EPSRC for the funding for his research studentship.

Appendix

Pauchard and Rica [1998] considered the contact of a spherical shell with a rigid plate. In the limit that the wall thickness, h , tends to zero, the situation before buckling is assumed to conform to configuration (I) of Figure 1, in which the top and bottom contact surface of the sphere flatten against the flat rigid plates, the plate having moved through a deflection, $2x$. When the shell has Young's modulus, E , and radius, R , the energy of this configuration has the form

$$U_I = \frac{c_0}{4} \frac{Eh^{5/2}}{R} x^{3/2} + c_1 \frac{Eh}{R} x^3. \quad (\text{A-1})$$

The first term is the energy of the axisymmetric fold and is deduced from the results for flat plates [Pauchard and Rica 1998; Ben and Pomeau 1997; Pomeau 1998]. The second term is the contribution from the compression of a portion of the sphere.

After buckling a section of the sphere inverts and the situation corresponds to Configuration II of Figure 1, which has energy given as

$$U_{II} = c_0 \frac{Eh^{5/2}}{R} x^{3/2} + c_2 \frac{Eh^3}{R} x. \quad (\text{A-2})$$

Here the first term is the contribution from the steeper axisymmetric fold and the second is due to the inversion of the spherical section by the flat surface. When x is small $U_I < U_{II}$ and Configuration I is energetically favourable. As x increases however, U_I increases faster than U_{II} (due to the x^3 dependence) and hence a point will be reached at which Configuration II is energetically more favourable and I is

unstable. This critical deformation corresponds to the energies being equal and thus depends on h and the parameters c_0 , c_1 and c_2 . The force in each of the configurations is given by the first derivatives of Equations (A-1) and (A-2), and is expected to be discontinuous at the transition for an experiment where the displacement increases monotonically. It is worth considering that the changes in the internal pressure as a result of the buckling are very small as a simple calculation of sphere volume shows that buckling introduces modest changes of only about 1% to the volume. The resulting pressure changes would have almost no contribution to the buckling forces.

The arguments leading to Equations (A-1) and (A-2) for the energies in the different configurations are essentially statements on the functional dependence of x from shell theory, hence the parameters c_0 , c_1 and c_2 , although dimensionless, can still be expected to depend on the material properties of the shell through Poisson's ratio, ν . In addition, these expressions strictly hold when the radius of the shell is much larger than the thickness and the deflections are larger than the fold radius of curvature.

Rather than derive the exact form of (A-1) and (A-2), this numerical investigation seeks to adopt the dimensionless approach of [Pauchard and Rica 1998]. Two hypotheses follow from this, which can be expressed in terms of the ratio of the deflection to the thickness ratio of the shell,

$$\varepsilon = x/h.$$

There is a critical value of ε at which buckling occurs, ε_b , which is the solution of a relation of the form

$$f(\varepsilon_b, \nu) = 0, \quad (\text{A-3})$$

where (in terms of the Pauchard parameters)

$$f(\varepsilon, \nu) = c_1(\nu)\varepsilon^3 - \frac{3}{4}c_0(\nu)\varepsilon^{3/2} - c_2(\nu)\varepsilon. \quad (\text{A-4})$$

By differentiating the expressions for the energy in each of the configurations, the functional dependence of the force, F , needed for a particular scaled deflection, ε , on the material and geometric parameters can be determined. In terms of the Young's modulus of the shell, E , its outer radius, R , and the shell thickness, h , this dependence is found to be

$$\frac{R}{Eh^3}F = \begin{cases} g_I(\varepsilon, \nu) & \text{if } \varepsilon < \varepsilon_b, \\ g_{II}(\varepsilon, \nu) & \text{if } \varepsilon > \varepsilon_b, \end{cases} \quad (\text{A-5})$$

and

$$g_I(\varepsilon, \nu) = \frac{3}{8}c_0(\nu)\varepsilon^{1/2} + 3c_1(\nu)\varepsilon^2, \quad g_{II}(\varepsilon, \nu) = \frac{3}{2}c_0(\nu)\varepsilon^{1/2} + c_2(\nu). \quad (\text{A-6})$$

References

- [Ben and Pomeau 1997] A. M. Ben and Y. Pomeau, "Crumpled paper", *Proc. R. Soc. Lond. A* **453**:1959 (1997), 729–755.
- [Föppl 1907] A. Föppl, *Vorlesungen über technische Mechanik, Bd. 5: die wichtigsten Lehren der höheren Elastizitätstheorie*, vol. 5, Teubner, Leipzig, 1907.
- [Kelly and Takhirov 2007] J. M. Kelly and S. M. Takhirov, "Tension buckling in multilayer elastomeric isolation bearings", *J. Mech. Mater. Struct.* **2**:8 (2007), 1591–1605.
- [Ketterling et al. 2007] J. A. Ketterling, J. Mamou, J. S. Allen III, O. Aristizábal, R. G. Williamson, and D. H. Turnbull, "Excitation of polymer-shelled contrast agents with high-frequency ultrasound", *J. Acoust. Soc. Am.* **121**:1 (2007), EL48–EL53.

- [Leong-Poi et al. 2002] H. Leong-Poi, J. Song, S. J. Rim, J. Christiansen, S. Kaul, and J. R. Lindner, “Influence of microbubble shell properties on ultrasound signal: implications for low-power perfusion imaging”, *J. Am. Soc. Echocardiogr.* **15**:10 (2002), 1269–1276.
- [Maalawi 2008] K. Y. Maalawi, “Optimal buckling design of anisotropic rings/long cylinders under external pressure”, *J. Mech. Mater. Struct.* **3**:4 (2008), 775–793.
- [Nakamura et al. 2004] K. Nakamura, M. Wada, S. Kuga, and T. Okano, “Poisson’s ratio of cellulose I β and cellulose II”, *J. Polym. Sci. B Polym. Phys.* **42**:7 (2004), 1206–1211.
- [Pauchard and Rica 1998] L. Pauchard and S. Rica, “Contact and compression of elastic spherical shells: the physics of a ‘ping-pong’ ball”, *Philos. Mag. B* **78**:2 (1998), 225–233.
- [Peng et al. 2000] H. X. Peng, Z. Fan, J. R. G. Evans, and J. J. C. Busfield, “Microstructure of ceramic foams”, *J. Eur. Ceram. Soc.* **20**:7 (2000), 807–813.
- [Pomeau 1998] Y. Pomeau, “Buckling of thin plates in the weakly and strongly nonlinear regimes”, *Philos. Mag. B* **78**:2 (1998), 235–242.
- [Taber 1983] L. A. Taber, “Compression of fluid-filled spherical shells by rigid indenters”, *J. Appl. Mech. (ASME)* **50**:4a (1983), 717–722.
- [Taguchi and Karushige 2007] I. Taguchi and M. Karushige, “Macroscopic elastic properties of randomly packed balloons”, *J. Mech. Mater. Struct.* **2**:3 (2007), 529–555.
- [Trivett et al. 2006] D. H. Trivett, H. Pincon, and P. H. Rogers, “Investigation of a three-phase medium with a negative parameter of nonlinearity”, *J. Acoust. Soc. Am.* **119**:6 (2006), 3610–3617.
- [Updike and Kalnins 1970] D. P. Updike and A. Kalnins, “Axisymmetric behaviour of an elastic spherical shell compressed between rigid plates”, *J. Appl. Mech. (ASME)* **37** (1970), 635–640.
- [Updike and Kalnins 1972] D. P. Updike and A. Kalnins, “Axisymmetric postbuckling and nonsymmetric buckling of a spherical shell compressed between rigid plates”, *J. Appl. Mech. (ASME)* **39** (1972), 172–178.
- [Wong and Pellegrino 2006a] Y. W. Wong and S. Pellegrino, “Wrinkled membranes, I: experiments”, *J. Mech. Mater. Struct.* **1**:1 (2006), 3–25.
- [Wong and Pellegrino 2006b] Y. W. Wong and S. Pellegrino, “Wrinkled membranes, III: numerical simulations”, *J. Mech. Mater. Struct.* **1**:1 (2006), 63–95.

Received 17 Oct 2008. Revised 15 Jun 2010. Accepted 8 Jul 2010.

ROBERT SHORTER: r.shorter@qmul.ac.uk

Department of Materials, Queen Mary University of London, Mile End Road, London, E1 4NS, United Kingdom

JOHN D. SMITH: jdsmith@dstl.gov.uk

Defence Science and Technology Laboratory, Porton Down, SP4 0JQ, United Kingdom

VINCENT A. COVENEY: vince.coveney@uwe.ac.uk

Engineering and Medical Technology Research Centre, University of the West of England, Bristol, BS16 1QY, United Kingdom

JAMES J. C. BUSFIELD: j.busfield@qmul.ac.uk

Department of Materials, Queen Mary University of London, Mile End Road, London, E1 4NS, United Kingdom

JOURNAL OF MECHANICS OF MATERIALS AND STRUCTURES

<http://www.jomms.org>

Founded by Charles R. Steele and Marie-Louise Steele

EDITORS

CHARLES R. STEELE Stanford University, U.S.A.
DAVIDE BIGONI University of Trento, Italy
IWONA JASIUK University of Illinois at Urbana-Champaign, U.S.A.
YASUhide SHINDO Tohoku University, Japan

EDITORIAL BOARD

H. D. BUI École Polytechnique, France
J. P. CARTER University of Sydney, Australia
R. M. CHRISTENSEN Stanford University, U.S.A.
G. M. L. GLADWELL University of Waterloo, Canada
D. H. HODGES Georgia Institute of Technology, U.S.A.
J. HUTCHINSON Harvard University, U.S.A.
C. HWU National Cheng Kung University, R.O. China
B. L. KARIHALOO University of Wales, U.K.
Y. Y. KIM Seoul National University, Republic of Korea
Z. MROZ Academy of Science, Poland
D. PAMPLONA Universidade Católica do Rio de Janeiro, Brazil
M. B. RUBIN Technion, Haifa, Israel
A. N. SHUPIKOV Ukrainian Academy of Sciences, Ukraine
T. TARNAI University Budapest, Hungary
F. Y. M. WAN University of California, Irvine, U.S.A.
P. WRIGGERS Universität Hannover, Germany
W. YANG Tsinghua University, P.R. China
F. ZIEGLER Technische Universität Wien, Austria

PRODUCTION

PAULO NEY DE SOUZA Production Manager
SHEILA NEWBERY Senior Production Editor
SILVIO LEVY Scientific Editor

Cover design: Alex Scorpan


Cover photo: Wikimedia Commons

See inside back cover or <http://www.jomms.org> for submission guidelines.

JoMMS (ISSN 1559-3959) is published in 10 issues a year. The subscription price for 2010 is US \$500/year for the electronic version, and \$660/year (+\$60 shipping outside the US) for print and electronic. Subscriptions, requests for back issues, and changes of address should be sent to Mathematical Sciences Publishers, Department of Mathematics, University of California, Berkeley, CA 94720-3840.

JoMMS peer-review and production is managed by EditFLOW™ from Mathematical Sciences Publishers.

PUBLISHED BY

 **mathematical sciences publishers**
<http://www.mathscipub.org>

A NON-PROFIT CORPORATION

Typeset in L^AT_EX

©Copyright 2010. Journal of Mechanics of Materials and Structures. All rights reserved.

- Axial compression of hollow elastic spheres** ROBERT SHORTER, JOHN D. SMITH,
VINCENT A. COVENEY and JAMES J. C. BUSFIELD 693
- Coupling of peridynamic theory and the finite element method**
BAHATTIN KILIC and ERDOGAN MADENCI 707
- Genetic programming and orthogonal least squares: a hybrid approach to
modeling the compressive strength of CFRP-confined concrete cylinders**
AMIR HOSSEIN GANDOMI, AMIR HOSSEIN ALAVI, PARVIN ARJMANDI,
ALIREZA AGHAEIFAR and REZA SEYEDNOUR 735
- Application of the Kirchhoff hypothesis to bending thin plates with different
moduli in tension and compression** XIAO-TING HE, QIANG CHEN, JUN-YI
SUN, ZHOU-LIAN ZHENG and SHAN-LIN CHEN 755
- A new modeling approach for planar beams: finite-element solutions based on
mixed variational derivations**
FERDINANDO AURICCHIO, GIUSEPPE BALDUZZI and CARLO LOVADINA 771
- SIFs of rectangular tensile sheets with symmetric double edge defects**
XIANGQIAO YAN, BAOLIANG LIU and ZHAOHUI HU 795
- A nonlinear model of thermoelastic beams with voids, with applications**
YING LI and CHANG-JUN CHENG 805
- Dynamic stiffness vibration analysis of thick spherical shell segments with variable
thickness** ELIA EFRAIM and MOSHE EISENBERGER 821
- Application of a matrix operator method to the thermoviscoelastic analysis of
composite structures** ANDREY V. PYATIGORETS, MIHAI O.
MARASTEANU, LEV KHAZANOVICH and HENRYK K. STOLARSKI 837